Human Reproduction, pp. 1–10, 2018
doi:10.1093/humrep/dex374

human reproduction

ORIGINAL ARTICLE *Reproductive biology*

Adipose tissue-derived stem cells in a fibrin implant enhance neovascularization in a peritoneal grafting site: a potential way to improve ovarian tissue transplantation

D.D. Manavella[1], L. Cacciottola[1,2], C.M. Desmet[3], B.F. Jordan[3], J. Donnez[4], C.A. Amorim[1], and M.M. Dolmans[1,5,*]

[1]Pôle de Recherche en Gynécologie, Institut de Recherche Expérimentale et Clinique, Université Catholique de Louvain, Avenue Mounier 52, bte. B1.52.02, 1200 Brussels, Belgium [2]Department of Biomedical Science for Health, Università degli Studi di Milano, Via Macedonio Melloni 52, 20125, Milan, Italy [3]Biomedical Magnetic Resonance Research Group, Louvain Drug Research Institute, Université Catholique de Louvain, Avenue Mounier 73, bte. B1.73.08, 1200 Brussels, Belgium [4]Society for Research into Infertility, Avenue Grandchamp 143, 1150 Brussels, Belgium [5]Gynecology Department, Cliniques Universitaires Saint-Luc, Avenue Hippocrate 10, 1200 Brussels, Belgium

*Correspondence address. Pôle de Recherche en Gynécologie, Institut de Recherche Expérimentale et Clinique, Université Catholique de Louvain, Avenue Mounier 52, bte B1.52.02, 1200 Brussels, Belgium. Tel: +32-02-764-5237; Fax: +32-02-764-9507; E-mail: marie-madeleine.dolmans@uclouvain.be

Submitted on August 22, 2017; resubmitted on November 16, 2017; accepted on December 11, 2017

STUDY QUESTION: Do two different concentrations of human adipose tissue-derived stem cells (ASCs) embedded inside a fibrin scaffold have the potential to differentiate into vessels and aid vascularization in a peritoneal grafting site intended for ovarian tissue transplantation?

SUMMARY ANSWER: Human ASCs in low and high concentrations differentiated into vessels when transplanted to mouse peritoneum inside a fibrin matrix, but only high ASC concentrations significantly increased human vessel area 14 days after transplantation.

WHAT IS KNOWN ALREADY: ASCs have multilineage differentiation potential, including proangiogenic properties and have been used in tissue engineering to enhance vascularization in transplanted tissues. Fibrin has been studied and used as an ASC-compatible biomaterial.

STUDY DESIGN, SIZE, DURATION: *In vivo* experimental model using 22 severe combined immunodeficient mice. In total, 16 mice (eight per group) were intraperitoneally grafted with a fibrin scaffold loaded with two different human ASC concentrations (either 150 000 [L-ASC] or 1 500 000 [H-ASC] cells) and lithium phthalocyanine (LiPc) crystals as oxygen-sensitive probes. Six mice were grafted with an empty fibrin (EF) implant containing only LiPc and served as controls. Levels of partial pressure of oxygen (pO_2) in implants were monitored *in vivo* by electron paramagnetic resonance oximetry (EPR). ASC identification, proliferation, and host and human vascularization were analyzed by immunohistochemistry (IHC). All analyses were performed on post-grafting Days 3, 7 and 14.

PARTICIPANTS/MATERIALS, SETTING, METHODS: Prospective experimental study conducted at the Gynecology Research Unit, Université Catholique de Louvain. All materials were used to perform pO_2 measurements (EPR oximetry), as well as histological (hematoxylin–eosin staining) and IHC (anti-human vimentin, anti-human Ki67, anti-mouse and human double CD34) analyses.

MAIN RESULTS AND THE ROLE OF CHANCE: A significant increase in pO_2 in implants was observed in all groups between Days 3 and 7 ($P < 0.001$). ASC-loaded implants displayed a tendency towards increased pO_2 levels from Days 7 to 14, not observed in EF implants. ASC-loaded implants showed differentiation into human CD34-positive vessels. Total CD34-positive endothelial area was correlated to pO_2 values obtained by EPR oximetry ($r = 0.6506$, $P = 0.0019$). In the H-ASC group, a greater human CD34-positive vascular surface area was found compared to the L-ASC group 14 days after transplantation ($P < 0.0049$).

LARGE SCALE DATA: N/A.

LIMITATIONS REASONS FOR CAUTION: As demonstrated by our results, ASCs transplanted inside a fibrin matrix can differentiate into CD34-positive human vessels. However, other possible mechanisms involved in ASC angiogenic behavior remain to be investigated.

WIDER IMPLICATIONS OF THE FINDINGS: High concentrations of ASCs loaded inside a fibrin scaffold could serve as a substrate to prepare a peritoneal grafting site over 14 days, in order to enhance vascularization once human ovarian tissue is grafted. Our proposed preparation of the grafting site would not only benefit ovarian tissue transplantation, but also other experimental avascular grafting procedures.

STUDY FUNDING/COMPETING INTEREST(S): This study was supported by grants from the Fonds National de la Recherche Scientifique de Belgique (FNRS-PDR Convention T.0077.14, Télévie Grant no. 7.6515.16F awarded to DDM and Grant 5/4/150/5 awarded to M.M.D. [CAA is FRS-FNRS research associate]), Fonds Spéciaux de Recherche, and Fondation St Luc, Foundation Against Cancer, and donations from the Ferrero family. None of the authors have any competing interests to declare.

Key words: adipose tissue-derived stem cells / fibrin / vascularization / ovarian tissue transplantation / EPR oximetry / grafting site / two-step transplantation

Introduction

Cancer in girls and young women has become increasingly curable over the past couple of decades (Donnez and Dolmans, 2013). However, while treatments are often highly effective for the underlying pathology, they can induce premature ovarian failure, leading to subsequent infertility (Donnez *et al.*, 2006). For patients undergoing these gonadotoxic treatments, several fertility preservation options are available: ovarian transposition, embryo cryopreservation, oocyte cryopreservation and ovarian tissue cryopreservation (Donnez *et al.*, 2006), the latter being the only alternative for prepubertal girls and patients who cannot delay treatment (Wallace *et al.*, 2014). Although more than 100 live births have been reported to date (Donnez *et al.*, 2015; Jensen *et al.*, 2016), early post-transplantation hypoxia remains an issue because of its negative impact on follicle survival (Van Eyck *et al.*, 2009, 2010), with follicle loss of >50% often observed during the first few days post-grafting (Baird *et al.*, 1999; Kim, 2006).

Increasing vascularization in grafted tissue is crucial, since it has been found to enhance follicle survival in mice (Shikanov *et al.*, 2011) and in human ovarian tissue (Xia *et al.*, 2015). A number of attempts have, therefore, been made to improve follicle survival rates in mouse models using both murine and human ovarian tissue (Mahmoodi *et al.*, 2014, 2015; Zhang *et al.*, 2015), with a view to increasing the efficiency of ovarian tissue transplantation.

Adipose tissue-derived stem cells (ASCs), first described by Zuk *et al.* (2001), constitute a population of mesenchymal stem cells (MSCs) with multiple mesodermal lineage capacities. The angiogenic potential of ASCs has been reported in a number of studies (De Francesco *et al.*, 2009; Veriter *et al.*, 2014), confirming their capacity to boost angiogenesis by secreting growth factors and allowing their differentiation into vessels (Moon *et al.*, 2006; Lafosse *et al.*, 2015). One group recently demonstrated that a combination of ASCs and adipose-derived microvascular endothelial cells embedded in fibrin and delivered in poly L-lactic acid/poly lactic-co-glycolic acid scaffolds favors vessel formation *in vitro* (before grafting) and enhances vascularization *in vivo* in the context of bioengineered muscle flaps for large soft tissue defects (Freiman *et al.*, 2016, 2017).

The aim of this study was to evaluate the role of ASCs in the angiogenic process and vascularization in a fibrin scaffold through ASC endothelial differentiation and proangiogenic behavior. We compared two different ASC concentrations delivered inside a fibrin scaffold grafted to mouse peritoneum for three different short-term periods, aiming to identify the best concentration of cells and most appropriate preparation time needed to optimize the ovarian tissue grafting site.

Materials and Methods

Experimental design

A total of 22 severe combined immunodeficient (SCID) mice were used for this experiment. In total, 16 mice (eight per group) were intraperitoneally grafted with a fibrin scaffold loaded with two different ASC concentrations (either $1.5.10^5$ or $1.5.10^6$ cells) and lithium phthalocyanine (LiPc) crystals (Dartmouth Medical School, Hanover, NH, USA). LiPc was used as an oxygen-sensitive paramagnetic probe, whose line-width is a linear function of partial pressure of oxygen (pO_2), and independent of local metabolic processes, other paramagnetic species, and pH. No toxic effect was detected in xenografted human ovarian tissue in a previous study by our group (Van Eyck *et al.*, 2009). Six mice were grafted with an empty fibrin (EF) implant containing only LiPc crystals and served as controls (Fig. 1).

Levels of pO_2 in implants were monitored *in vivo* on post-grafting Days 3 ($n = 14$), 7 ($n = 16$) and 14 ($n = 8$) by electron paramagnetic resonance oximetry (EPR), as previously described (Van Eyck *et al.*, 2009). Two or three mice from each group were killed after each measurement and implants were collected for histology and immunohistochemistry (IHC) (Fig. 1).

Adipose tissue-derived stem cells

Human ASCs from female donors were commercially acquired (STEMPRO® human ASCs, Invitrogen, Carlsbad, CA, USA). These cells were shown to express a flow cytometry cell surface protein profile positive for CD29, CD44, CD73, CD90, CD105 and CD166 (>95%), but negative for CD34, CD14, CD31, CD45 and Lin1 (<2%), consistent with specific surface antigen criteria that characterize MSCs (Dominici *et al.*, 2006).

ASCs were cultured and expanded at 37°C in 5% CO_2/95% air in MesenPRO RS medium (Gibco, Glasgow, Scotland), supplemented with 2% *v/v* MesenPRO RS growth supplement (Gibco), 1% *v/v* L-glutamine (Gibco) and 1% *v/v* penicillin–streptomycin (Gibco). Cultures were washed in phosphate-buffered saline (PBS, Gibco) and passaged by enzymatic digestion using Accutase (Sigma-Aldrich, St. Louis, Missouri, USA) after achieving a density of 80–90%. Repeated viability tests with addition of trypan blue solution (Sigma-Aldrich) showed very high (~95%) viability. Cells used in this study were all between passages 2 and 5.

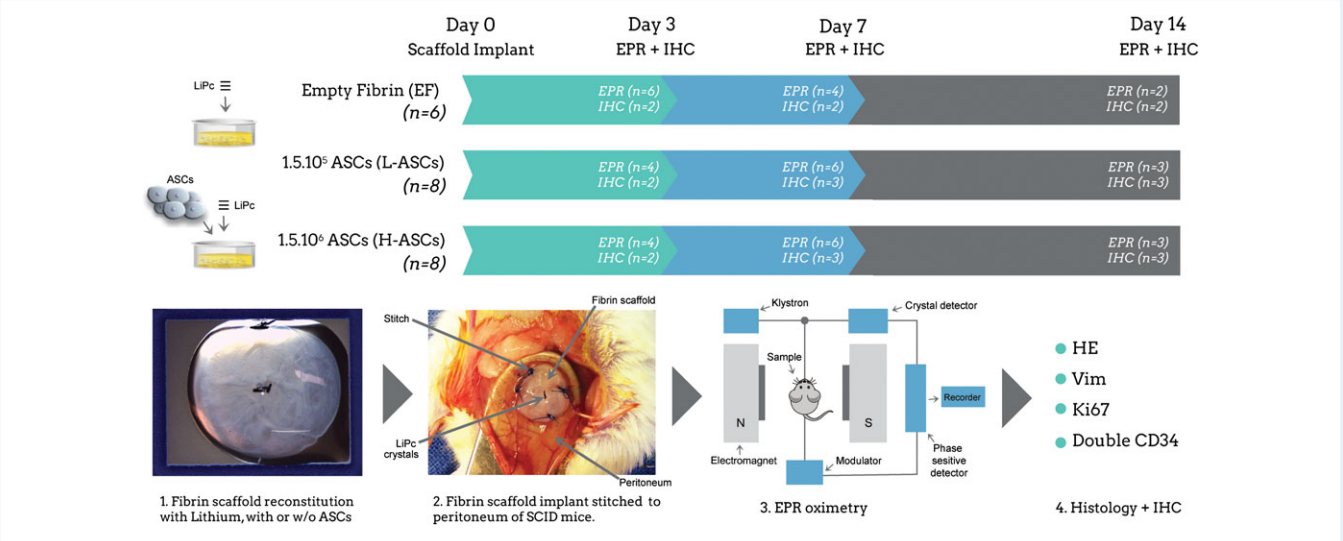

Figure 1 Twenty-two SCID mice were intraperitoneally grafted with a fibrin scaffold loaded with two different adipose tissue-derived stem cells (ASC) concentrations (low 1.5×10^5 and high 1.5×10^6 cells) and lithium phthalocyanine (LiPc) crystals, while empty fibrin (EF) implants containing only LiPc were grafted to controls. Electron paramagnetic resonance (EPR) oximetry was performed on Days 3, 7 and 14 before euthanizing the animals for histology and immunohistochemical assessments in a staggered fashion. Vim: anti-human vimentin.

Incorporation of cells into fibrin implants and LiPc crystal insertion

Fibrin scaffolds were assembled as previously described (Chiti *et al.*, 2016), with volume and concentrations of fibrinogen and thrombin determined according to preliminary studies. A volume of 22.5 µL of fibrinogen solution (50 mg/mL) (Tisseel, Baxter, Belgium) was placed in 8-well glass chamber slides. One-hundred and fifty thousand ASCs (low concentration [L-ASCs]) (75 µL fibrin, 10^4 cells/µL) or $1.5.10^6$ ASCs (high concentration [H-ASCs]) (75 µL fibrin, 10^5 cells/µL) (Germain *et al.*, 2015) suspended in 15 µL of growth medium were successively added to the fibrinogen, while 15 µl of growth medium without cells was added to the controls. The fibrinogen solution containing the medium with or without cells was mixed with thrombin (50 IU/mL) at a *v:v* ratio of 1:1. Two to three LiPc crystals were then placed inside the fibrin scaffolds using small forceps, prior to incubation for 15–30 min at 37°C for fibrin polymerization. The implants were then gently detached for xenografting.

Ethical approval

Animal welfare guidelines were approved by the Committee on Animal Research of the Université Catholique de Louvain.

Transplantation procedure

A total of 22 female SCID mice (Charles River Laboratories, France) were used for this study. Satisfactory housing and breeding conditions, anesthesia and analgesia were achieved as previously reported (Nisolle *et al.*, 2000). A horizontal incision was made in the skin and abdominal wall to attach the implants to the lower third of the parietal peritoneum. The inner peritoneal surface was scratched with a scalpel (Luyckx *et al.*, 2014), before gently suturing the scaffold with 2–3 cardinal stitches using 7/0 Prolene. Each mouse was grafted with a scaffold containing H-ASCs or L-ASCs plus LiPc crystals ($n = 16$). The remaining control mice ($n = 6$) were grafted with EF implants containing only LiPc crystals. The abdominal wall and skin were then closed.

EPR oximetry

EPR oximetry is a sensitive, non-invasive method that allows repeated *in vivo* measurements of tissue pO_2 with an accuracy of <1 mmHg (Van Eyck *et al.*, 2009). The extent of the effect is related to the amount of oxygen present in the environment of the paramagnetic materials (Khan *et al.*, 2007). EPR spectra were recorded using an EPR spectrometer (Clin-EPR, Dartmouth EPR Center, Lebanon, NH, USA) with a low-frequency microwave bridge operating at 1.15 GHz and an extended loop resonator. Typical spectrometer parameters included scan range of 0.25 mT, scan time of 3 s, 1024 points/scan, modulation amplitude of 0.01 mT, incident microwave power of 0.794 mW, modulation frequency of 21.3 kHz and accumulation of 20–30 scans per measurement. For pO_2 measurements, the mice were anesthetized using isoflurane (3% for induction, 2% for maintenance) with strictly controlled air-breathing movements. Body temperature was maintained by use of a heated water blanket. The mice were positioned in the center of the magnet so that the graft site containing LiPc crystals was directly under the extended loop resonator. EPR line-widths (LW) were converted to pO_2 by means of a calibration curve determined for the LiPc crystals used in this study. The pO_2 was calculated using the following equation: $y = 0.0371x + 0.0161$ [y = LW (G) and x = % O_2; 100% O_2 = 760 mmHg].

Monitoring of pO_2 was performed on post-grafting Days 3, 7 and 14. After exposure to ambient air-breathing conditions (21% O_2), negative controls were applied to confirm the oxygen sensitivity of the paramagnetic probes for each mouse. For these negative controls, pO_2 levels were measured reproducibly 15 min after the mice were euthanized by cervical dislocation (0% O_2).

Histological and immunohistochemical staining

All recovered samples were fixed in 4% formaldehyde, embedded in paraffin and serially sectioned (5-µm-thick coronal sections from the fibrin component to the peritoneum). The slides were stained with hematoxylin–eosin (HE) (Merck, Darmstadt, Germany) for histological evaluation, digitized after

immunolabeling using the Mirax Scan system (Zeiss, Germany), and analyzed using Mirax Viewer or ImageJ (http://rsb.info.nih.gov/ij/) software.

To assess fibrin resorption kinetics, the volume of the implants was investigated by applying the Cavalieri principle. Serial HE-stained sections were evaluated every 60 µm using ×4 magnification, and analyzed with ImageJ to count the points superimposed on fibrin implant images. Total volume (mm^3) was estimated using the following equation:

$$V_{tot} = \sum_{i=1}^{n} P \times a(P) \times t$$

where $\sum_{i=1}^{n} P$ is the total number of points, $a(P)$ is the corresponding area of each point and t is the distance between sampled sections and section thickness (Mahmoodi *et al.*, 2014).

Identification and proliferation of implanted ASCs

Vimentin, a cytoskeletal protein, is a marker of cells of mesenchymal origin. In order to label and identify grafted ASCs and quantify the number of proliferating ASCs, anti-human vimentin and Ki67 immunostaining respectively were performed, as previously reported (Soares *et al.*, 2015). Primary antibodies used were mouse anti-human vimentin (1:1000 dilution, clone V9, 0725, Dako) and mouse anti-human Ki67 (1:100 dilution, clone MIB, mAb ref.: M7240, Dako). The secondary antibody used was Envision goat anti-mouse IgG (1:2 dilution, Dako). For negative controls, slides were incubated without the primary antibodies. One section per implant was stained and analyzed for vimentin and three for Ki67. After delimiting the implant, the proportion of vimentin-positive surface area was calculated, as well as the number of proliferating cells.

Implant vascularization

Vessels of both murine and human origin were investigated by double CD34 immunolabeling, staining endothelial cell membranes, as detailed in an earlier publication (Soares *et al.*, 2015). Antibodies used were rat anti-mouse CD34 (1:100 dilution, clone MEC 14.7, HM 1015; Hycult Biotechnology, Uden, the Netherlands) and rabbit anti-rat coupled to biotin, followed by mouse anti-human CD34 (1:500 dilution, clone QBEnd/10, CM084B; Biocare Medical, Concord, CA) and goat anti-mouse (1:300 dilution; Jackson Immunoresearch, Suffolk, UK). Nuclei were counterstained with hematoxylin. For negative controls, one slide was incubated without the primary antibodies. Six sections per graft were analyzed after dividing the implants into two distinct areas in order to further identify the optimal surface for ovarian tissue grafting: (i) the area of the implant in direct contact with the peritoneum and delimited by the stitches, namely the contact zone (CZ) or (ii) the area corresponding to non-resorbed fibrin. Vessel sections were considered positive when at least one endothelial cell was stained. Results are expressed as the percentage of surface area covered with vessels, or endothelial area relative to total section area.

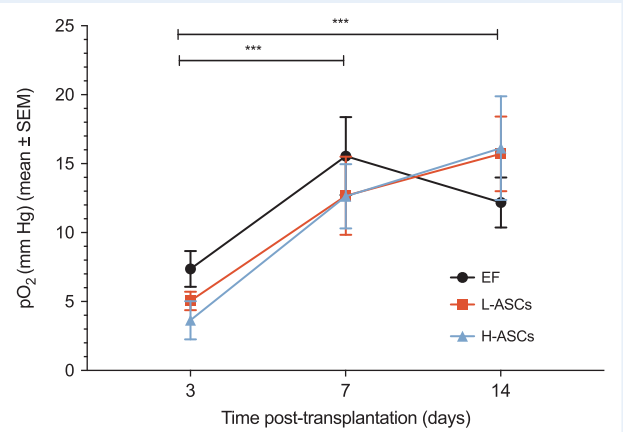

Figure 2 Monitoring of pO_2 values shown in millimeters of mercury (mmHg) (mean ± SEM, $n = 20$, two-way ANOVA and Tukey's post-hoc test). Values increased significantly from Days 3 to 7 (***$P = 0.0008$) in all groups. EF, empty fibrin; L-ASCs, low adipose tissue-derived stem cell (ASC) concentration (1.5×10^5 cells); H-ASCs, high ASC concentration (1.5×10^6 cells).

Statistical analysis

Results are expressed as means ± SEM. GraphPad Prism, version 7.00 for Windows (GraphPad Software, La Jolla, CA, USA), was used for statistical analyses. Two-way ANOVA followed by Tukey's multiple comparison test and uncorrected Fisher's LSD test were applied where appropriate. A P-value <0.5 was considered statistically significant. Linear regression was performed to correlate endothelial area with pO_2 values.

Results

EPR oximetry

Use of EPR in a fibrin scaffold

The responsiveness of LiPc crystals to pO_2 variations may be lost over time depending on implantation site. For this reason, and given the fact that no information is available on LiPc stability in fibrin scaffolds, negative control measurements were included to ascertain the responsiveness of the paramagnetic probe to pO_2 variations.

Results of negative controls confirmed the responsiveness of LiPc to pO_2, following clear changes in pO_2 conditions.

A significant decrease in pO_2 levels was observed 15 min after euthanasia compared to ambient air-breathing conditions (mean pO_2 ± SD: 8.66 ± 1.38 mmHg and 3.42 ± 0.52 mmHg [$P = 0.0049$] for ambient air-breathing conditions [21% O_2] and post-mortem measurements [0% O_2], respectively).

pO_2 monitoring in fibrin implants

Levels of pO_2 were monitored and analyzed in 20 of the 22 operated mice (Fig. 2). Two mice were excluded because no measurable LiPc values were obtained, suggesting spatial dispersion or disruption of the crystals, which could create signal interference and loss of sensitivity in measurements (Desmet *et al.*, 2015). Indeed, one of the recovered implants had LiPc crystals dispersed throughout the fibrin scaffold, and the other showed LiPc crystals located in fatty tissue surrounding the grafting site. A significant increase in pO_2 was observed in all groups between Days 3 and 7 ($P = 0.0008$), but no significant difference was found from Days 7 to 14. However, ASC-loaded implants showed a tendency towards increased pO_2 levels from Days 7 to 14 (mean pO_2: L-ASCs: 12.67 mmHg on Day 7 and 15.71 mmHg on Day 14; H-ASCs: 12.62 mmHg on Day 7 and 16.12 mmHg on Day 14), unlike EF implants (mean pO_2: EF: 15.54 mmHg on Day 7 and 12.18 on Day 14 mmHg). No significant difference was detected between groups at any individual time point.

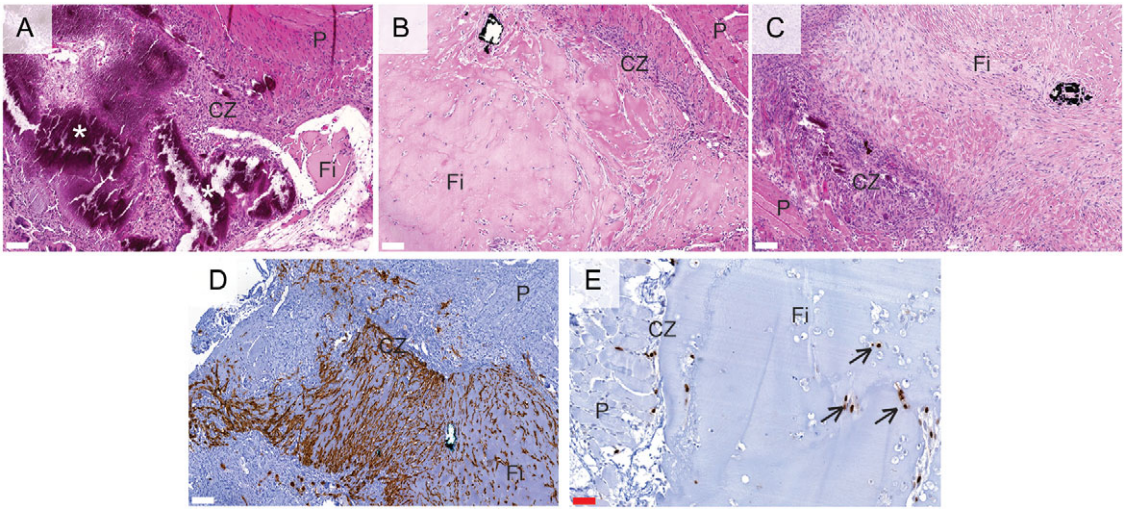

Figure 3 (**A**) Haematoxylin and eosin (HE) staining showing necrotic-like areas (asterisks) in the empty fibrin (EF) group on Day 14. HE staining on Day 14 in low (1.5×10^5) adipose tissue-derived stem cells (L-ASCs) (**B**) and high (1.5×10^6) ASC (H-ASCs) (**C**). Specific anti-human vimentin (**D**) and Ki67 (**E**) Immunohistochemistry of the H-ASC group on Days 14 and 3, respectively. Arrows: proliferating cells. EF, empty fibrin; CZ, contact zone; Fi, non-resorbed fibrin; P, peritoneum. White scale bar: 100 μm, red scale bar: 50 μm.

Macroscopic, histological and immunohistochemical evaluation

Macroscopic evaluation

The implant recovery rate was 100%. On Day 3, EF implants had a white appearance and adhered to the peritoneum only by means of stitches, as fibrin could be easily detached from the peritoneum in central areas where stitches had not been placed. ASC-loaded implants (L-ASCs and H-ASCs), however, were more adherent to the peritoneum. By Day 7 and up to Day 14, all implants were adherent to the peritoneum across the entire fibrin surface and had a more transparent appearance in the H-ASC and L-ASC groups than in the EF group.

Microscopic evaluation

Implant resorption was assessed by estimating the volume of retrieved implants in HE-stained sections (Fig. 3A–C). Implants showed progressive fibrin resorption over time in all groups (Table 1), but no difference between groups at any time point.

At histological analysis, necrotic-like areas were observed on HE slides, consisting of intensely basophilic areas in the fibrin that reached 18% of implants in the EF group (Fig. 3A), but accounted for <2% of implant surface area in the H-ASC and L-ASC groups (Fig. 3B, C) (Table 1).

ASC identification and proliferation in ASC-loaded implants

Anti-human vimentin IHC (Fig. 3D) showed a tendency towards increased area occupied by ASCs over time with both ASC concentrations. The largest area occupied by human vimentin-positive ASCs was found in the H-ASC group on Day 7 (mean percentage: area 16.23% of the implant) (Table 1).

Proliferation of grafted human ASCs evaluated by anti-human Ki67 IHC (Fig. 3E) appeared to decrease in proliferating ASCs in the H-ASC group (number of Ki67-positive cells/mm^2) from Days 3 to 14, while the L-ASC group showed no significant difference in proliferation over time (Table 1).

Implant vascularization

Regarding non-resorbed fibrin area vascularization, human and murine CD34-positive vessels evaluated by endothelial area (Fig. 4A–F) showed a significant increase over time in the H-ASC group ($P = 0.005$), but not in the L-ASC group, where no significant difference was observed ($P = 0.34$) (Fig. 5A).

In terms of CZ vascularization, there was an apparent increase in total endothelial area between Days 3 and 7 in all groups, but only the L-ASC group showed a significant increase between Days 7 and 14 (L-ASCs: $P = 0.01$) (Fig. 5A). No difference was noted between groups at any individual time point.

Human CD34-positive vessels were detected in both CZ and non-resorbed fibrin areas of implants in the H-ASC and L-ASC groups (Fig. 5B). In terms of non-resorbed fibrin area, there was a significant increase from Days 7 to 14 in human endothelial area in the H-ASC group ($P = 0.0006$). A significant difference was found on Day 14 between the L-ASC group and the H-ASC group ($P = 0.0049$). The largest human CD34-positive surface area was observed in the H-ASC group. With respect to CZ area, there was no significant difference in human endothelial area over time, nor between groups. A positive correlation was found when comparing total endothelial area with pO_2 values obtained by EPR oximetry ($r = 0.6506$, $P = 0.0019$) (Fig. 5C).

Discussion

The present study was designed to evaluate the impact of preparing a peritoneal grafting site using two different concentrations of ASCs embedded in fibrin implants, with a view to potential future

Table I Post-grafting implant outcomes

	Analysis	Group (*n*/day 3-*n*/day 7-*n*/day14)	Day 3	Day 7	Day 14
A	Fibrin volume (mm^3)	EF (2-2-2)	14.4 ± 1.24	3.2 ± 0.31	2.1 ± 0.11
		L-ASCs (2-3-3)	14.4 ± 0.32	6.0 ± 1.30[a]	0.9 ± 0.21[a]
		H-ASCs (2-3-3)	14.9 ± 0.49	4.7 ± 0.86[b]	1.4 ± 0.27[b]
B	Necrotic-like areas (%)	EF (2-2-2)	0.2 ± 0.06	7.4 ± 1.37[c,d,e]	18.4 ± 0.78[c,f,g]
		L-ASCs (2-3-3)	0.1 ± 0.13	0.08 ± 0.07[d,h]	1.1 ± 1.18[f,h]
		H-ASCs (2-3-3)	0.00 ± 0.00	0.5 ± 0.46[e]	1.0 ± 0.36[g]
C	Human vimentin-positive surface area (%)	L-ASCs (2-3-3)	3.1 ± 0.78	3.9 ± 1.72[i]	10.9 ± 6.20
		H-ASCs (2-3-3)	6.5 ± 4.77	16.2 ± 1.05[i]	15.1 ± 4.15
D	Human Ki67-positive cells (No. of Ki67-positive cells/mm^2)	L-ASCs (2-3-3)	60.7 ± 2.55	23.8 ± 9.46	24.5 ± 13.26
		H-ASCs (2-3-3)	121.3 ± 0.00[j]	55.3 ± 31.55	21. 2 ± 7.39[j]

(A) Implant volume according to Cavalieri's principle to evaluate implant resorption over time (Two-way ANOVA and Tukey's post-hoc test). $^{a\neq a}P < 0.001$, $^{b\neq b}P = 0.0154$. (B) Necrotic-like percentage area in implants (Two-way ANOVA and Tukey's post-hoc test). Letters c-h represent: $P < 0.0001$. (C) Anti-human vimentin IHC to assess ASC-covered surface area (Two-way ANOVA and Fisher's LSD post-hoc test). $^{i\neq i}P < 0.0391$. (D) Anti-human Ki67 IHC to assess the number of proliferating cells per mm^2 (Two-way ANOVA and Fisher's LSD post-hoc test). $^{j\neq j}P < 0.0169$. EF, empty fibrin; L-ASCs, low ASC concentration (1.5×10^5 cells); H-ASCs, high ASC concentration (1.5×10^6 cells). For L-ASC and H-ASC groups, *n* was 2 on Day 3 and 3 on Days 7 and 14.

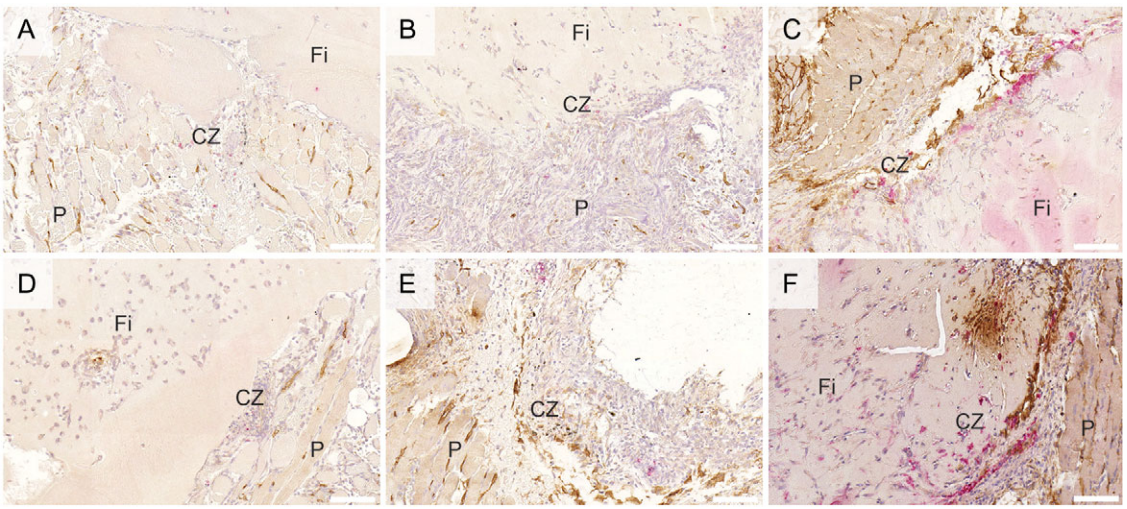

Figure 4 Double CD34 immunostaining of human and murine vascular structures using species-specific antibodies as endothelial cell markers (merged red and brown image; red: human-specific CD34, brown: mouse-specific CD34). (**A–C**) low (1.5×10^5) adipose tissue-derived stem cells (L-ASC) group on days 3 (A), 7 (**B**) and 14 (**C**). (**D–F**) high (1.5×10^6) ASC (H-ASC) group on Days 3 (D), 7 (E) and 14 (**F**). CZ, contact zone; Fi, non-resorbed fibrin; P, peritoneum. White scale bar: 100 μm

application in ovarian tissue transplantation. To our knowledge, this is the first time that EPR oximetry has been applied to investigate *in vivo* oxygenation kinetics inside a fibrin scaffold implanted in the peritoneal cavity with or without ASCs. This technique enabled us to establish how a fibrin implant becomes vascularized over time when grafted to the peritoneum of SCID mice. In a comparison of oxygenation kinetics, we found a similar tendency in all groups, regardless of the presence of ASCs, showing an increase over the first 7 days and no difference up to Day 14. Our oxygenation curve exhibited the same pattern as observed previously (Van Eyck *et al.*, 2009) in ovarian tissue, with values climbing over the course of the first 10 days. The increase in pO_2 suggests an active process of implant vascularization, resulting in subsequently improved oxygenation.

Progressive vascularization of the fibrin implants was evaluated by immunolabeling the CD34 antigen of both human and murine origin. Results obtained for total endothelial area showed that the area in direct contact with the peritoneum (CZ), which is the first to be reached by host vessels, has a larger vascularized surface. We observed not only host vessels contributing to the vascularization of fibrin implants, but also newly formed human vessels, as CD34-positive human vessels were found in both areas of the implant. Areas covered with human

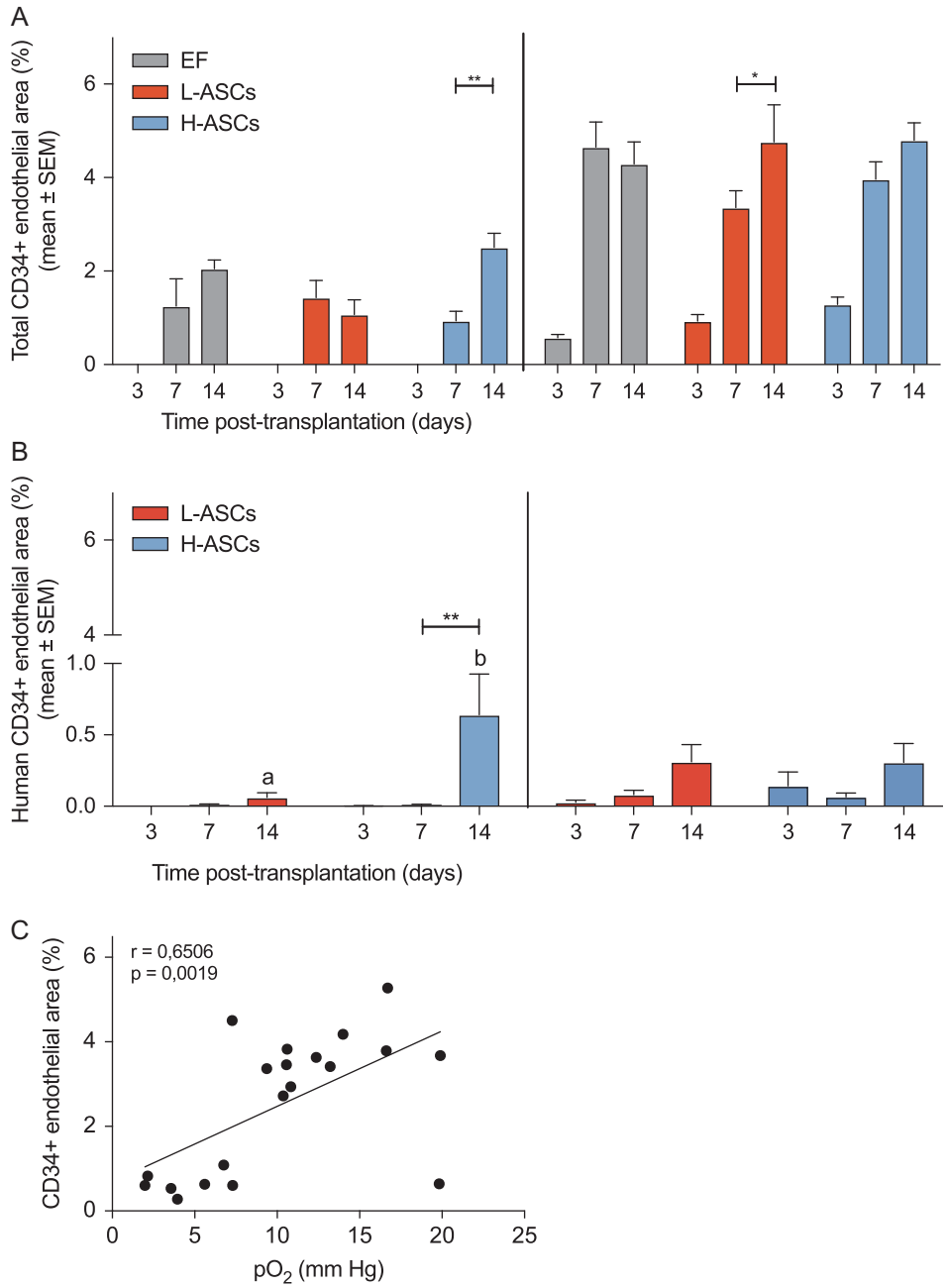

Figure 5 (**A**) Total endothelial area (EA) by double CD34 immunohistochemistry (IHC) to assess the percentage of vessel-covered surface area. (**B**) Human EA by anti-human CD34 IHC to evaluate the percentage of human vessel-covered surface area (mean ± SEM, two-way ANOVA and Fisher's LSD post-hoc test). (**C**) Correlation between EA and pO_2 expressed as a percentage of surface area and in millimeters of mercury (mmHg) respectively. *P*-value references: $^{*}P < 0.05$, $^{**}P < 0.01$, $^{a\neq b}P = 0.0049$. EF, empty fibrin; L-ASCs, low ASC concentration (1.5×10^5 cells); H-ASCs, high ASC concentration (1.5×10^6 cells).

vessels were similar in both non-resorbed fibrin and CZ regions, but greater in the non-resorbed fibrin region in the H-ASC group, suggesting that endothelial differentiation of ASCs is directly proportional to the number of grafted ASCs.

Our results on double CD34 immunostaining are consistent with previous observations by Germain *et al.* (2015) on SCAP cells and Chiti *et al.* (2017) in the context of the transplantable artificial ovary model, showing host endothelial cell infiltration and vascularization of fibrin implants.

Our findings suggest that the number of cells used could play a role and may well be important for the formation of human neovessels (Rubina *et al.*, 2009), since human vessels detected in fibrin covered a greater surface area in implants loaded with high concentrations of ASCs. The positive angiogenic behavior of ASCs in this study

corroborated previous findings with ASCs (Chung et al., 2015) and mesenchymal precursor cells (Koike et al., 2004).

One of the main mechanisms that may explain our findings is differentiation of MSCs into endothelial cells and pericytes, thereby providing the necessary cellular components to stabilize newly formed vessels (Au et al., 2008; De Francesco et al., 2009; Mendel et al., 2013). ASC differentiation is also supported by the significant decrease in cell proliferation in the H-ASC group over time, suggesting that ASCs may undergo a proliferation/differentiation switch (Garcia et al., 1999; Conti et al., 2001; Chen et al., 2006).

According to the literature, MSCs promote vascular formation through secretion of growth factors such as VEGF, FGF2, HGF, bFGF, PDGFB, TGFβ and angiogenin among others, mainly secreted when exposed to hypoxia (Rubina et al., 2009), which have proven to promote angiogenesis (Chung et al., 2015; Xia et al., 2015). This important mechanism could also explain the differences observed in our study.

ASC-loaded fibrin scaffolds had a better macroscopic and microscopic appearance, showing significantly fewer necrotic-like areas in HE-stained sections than implants without ASCs. The low degree of this inflammatory pattern in implants containing ASCs suggests their protective role, not witnessed in implants without cells. ASCs may play a part in modulating host activation with respect to the graft and inflammation, as it is known that they can modify and inhibit the innate immune response (Castro-Manrreza and Montesinos, 2015).

Regarding the presence of grafted cells inside the fibrin implants, it appears that a large number of ASCs remained in the grafting site, as they were still detectable by anti-human vimentin IHC and accounted for up to 16% of implants by Day 14 in our model. This was not the case in other studies, where ASCs that were intravenously injected or locally transplanted sustained massive cell loss (Sun et al., 2013; Su et al., 2016). Based on these findings, we could hypothesize that ASCs may not undergo solely endothelial differentiation, as the percentage of surface area covered with human CD34-positive vessels reached 1% of implants in the H-ASC group. The difference in observed percentages not only suggests differentiation into other cell types of mesenchymal lineage, such as fibroblasts (Hong et al., 2013), but also retention of stemness after 14 days.

Subjecting patients to a two-step procedure for fertility restoration, using ASCs in a first step to prepare the ovarian tissue transplantation site, may be justified if a significant increase in follicle survival rates can be achieved. Indeed, the first live birth from human ovarian tissue cryopreservation and transplantation published by Donnez et al. (2004) was obtained by means of two surgical procedures. The first involved creation of a peritoneal window and coagulation of its edges to improve neoangiogenesis. After 7 days, ovarian tissue was transplanted to this specially created peritoneal window, where an extensive vascular network was visible (Donnez et al., 2004).

We chose ASCs for our model because of their easy harvesting in large numbers using minimally invasive procedures like liposuction. However, there is also evidence that ASCs retain their phenotypic and functional characteristics after long-term cryopreservation (Yong et al., 2015), which would allow cell harvesting as soon as human ovarian tissue is retrieved from patients. Although commercial ASCs were used for this study, autologous ASCs would be employed for clinical applications.

Another supporting argument is the number of existing therapies already using ASCs in a variety of fields, such as rheumatology (Garimella et al., 2015), gastroenterology (Lee et al., 2013), neurology (Staff et al., 2016), and plastic and reconstructive surgery for chronic wound healing and bone regeneration (Veriter et al., 2015). Moreover, numerous clinical trials (phases I–II and III) assessing ASC safety and efficacy are currently being conducted or have already been completed (https://clinicaltrials.gov: 214 ongoing, 57 completed), testifying to the widespread interest in the potential of these cells.

This study could serve as a starting point for further investigations to determine the kinetics of oxygen diffusion in fibrin-based biomaterials, as no studies have yet been published on the influence of biophysical properties of different fibrin formulations and their impact on the ability of oxygen molecules to navigate throughout the scaffold.

We believe that our proposed preparation of the grafting site would not only benefit ovarian tissue transplantation, but also other experimental avascular grafting procedures, such as the artificial ovary made from fibrin formulations (Chiti et al., 2016, 2017).

Conclusion

We investigated and demonstrated the effectiveness of EPR oximetry to evaluate the oxygen environment in a fibrin scaffold transplanted to mouse peritoneum. We observed that pO_2 values obtained by EPR correlate strongly with implant vascularization, confirming its valuable role in O_2 monitoring of fibrin grafts. High ASC concentrations were found to increase human vessel area over time. The ability of ASCs to promote human neoangiogenesis by differentiation and growth factor secretion appears to be dependent on both cell concentration and time. We therefore conclude that ASCs loaded inside a fibrin scaffold at high concentrations could serve as a substrate to prepare the grafting site over 14 days, in order to enhance vascularization once human ovarian tissue is grafted. Our study constitutes an important first step towards improving the transplantation site for avascular grafting procedures by applying a novel technique that may some day be used for ovarian tissue transplantation. Future studies will need to investigate the effect of this approach on follicle survival rates and graft vascularization.

Acknowledgements

The authors thank Mira Hryniuk, BA, for reviewing the English language of the article, and Dolores Gonzalez, Olivier Van Kerk and Guillaume Courtoy for their technical assistance.

Authors' roles

D.D.M.: Experimental design, experimental procedures, analyses, statistical analysis, interpretation of results and article preparation. L.C.: Experimental procedures, analyses, statistical analysis and participation in article preparation. C.M.D.: EPR oximetry. B.F.J.: EPR oximetry and article revision. J.D.: Article preparation and revision. C.A.A.: Article preparation and revision. M.M.D.: Experimental design, experimental procedures, interpretation of results and article revision.

Funding

Grants from the Fonds National de la Recherche Scientifique de Belgique (Fonds National de la Recherche Scientifique de Belgique-Projet de Recherche (FNRS-PDR) Convention T.0077.14, Télévie Grant no. 7.6515.16F awarded to D.D.M., Grant 5/4/150/5 awarded to M.M.D. and C.A.A. is Fonds de Recherche Scientifique (FRS)-FNRS research associate), Fonds Spéciaux de Recherche, and Fondation St Luc, Foundation Against Cancer, and donations from the Ferrero family.

Conflict of interest

None of the authors have any competing interests to declare in relation with this subject.

References

Au P, Tam J, Fukumura D, Jain RK. Bone marrow-derived mesenchymal stem cells facilitate engineering of long-lasting functional vasculature. *Blood* 2008;**111**:4551–4558.

Baird DT, Webb R, Campbell BK, Harkness LM, Gosden RG. Long-term ovarian function in sheep after ovariectomy and transplantation of autografts stored at −196°C. *Endocrinology* 1999;**140**:462–471.

Castro-Manrreza ME, Montesinos JJ. Immunoregulation by mesenchymal stem cells: biological aspects and clinical applications. *J Immunol Res* 2015;**2015**:394917.

Chen JF, Mandel EM, Thomson JM, Wu Q, Callis TE, Hammond SM, Conlon FL, Wang DZ. The role of microRNA-1 and microRNA-133 in skeletal muscle proliferation and differentiation. *Nat Genet* 2006;**38**: 228–233.

Chiti MC, Dolmans MM, Lucci CM, Paulini F, Donnez J, Amorim CA. Further insights into the impact of mouse follicle stage on graft outcome in an artificial ovary environment. *Mol Hum Reprod* 2017;**23**:381–392.

Chiti MC, Dolmans MM, Orellana R, Soares M, Paulini F, Donnez J, Amorim CA. Influence of follicle stage on artificial ovary outcome using fibrin as a matrix. *Hum Reprod* 2016;**31**:427–435.

Chung E, Rytlewski JA, Merchant AG, Dhada KS, Lewis EW, Suggs LJ. Fibrin-based 3D matrices induce angiogenic behavior of adipose-derived stem cells. *Acta Biomater* 2015;**17**:78–88.

Conti L, Sipione S, Magrassi L, Bonfanti L, Rigamonti D, Pettirossi V, Peschanski M, Haddad B, Pelicci P, Milanesi G *et al*. Shc signaling in differentiating neural progenitor cells. *Nat Neurosci* 2001;**4**:579–586.

De Francesco F, Tirino V, Desiderio V, Ferraro G, D'Andrea F, Giuliano M, Libondi G, Pirozzi G, De Rosa A, Papaccio G. Human CD34/CD90 ASCs are capable of growing as sphere clusters, producing high levels of VEGF and forming capillaries. *PLoS One* 2009;**4**:e6537.

Desmet CM, Lafosse A, Veriter S, Porporato PE, Sonveaux P, Dufrane D, Leveque P, Gallez B. Application of electron paramagnetic resonance (EPR) oximetry to monitor oxygen in wounds in diabetic models. *PLoS One* 2015;**10**:e0144914.

Dominici M, Le Blanc K, Mueller I, Slaper-Cortenbach I, Marini F, Krause D, Deans R, Keating A, Prockop D, Horwitz E. Minimal criteria for defining multipotent mesenchymal stromal cells. The International Society for Cellular Therapy position statement. *Cytotherapy* 2006;**8**:315–317.

Donnez J, Dolmans MM. Fertility preservation in women. *Nat Rev Endocrinol* 2013;**9**:735–749.

Donnez J, Dolmans MM, Demylle D, Jadoul P, Pirard C, Squifflet J, Martinez-Madrid B, van Langendonckt A. Livebirth after orthotopic transplantation of cryopreserved ovarian tissue. *Lancet* 2004;**364**:1405–1410.

Donnez J, Dolmans M-M, Diaz C, Pellicer A. Ovarian cortex transplantation: time to move on from experimental studies to open clinical application. *Fertil Steril* 2015;**104**:1097–1098.

Donnez J, Martinez-Madrid B, Jadoul P, Van Langendonckt A, Demylle D, Dolmans MM. Ovarian tissue cryopreservation and transplantation: a review. *Hum Reprod Update* 2006;**12**:519–535.

Freiman A, Shandalov Y, Rosenfeld D, Shor E, Ben-David D, Meretzki S, Levenberg S, Egozi D. Engineering vascularized flaps using adipose-derived microvascular endothelial cells and mesenchymal stem cells. *J Tissue Eng Regen Med* 2017 [Epub ahead of print].

Freiman A, Shandalov Y, Rozenfeld D, Shor E, Segal S, Ben-David D, Meretzki S, Egozi D, Levenberg S. Adipose-derived endothelial and mesenchymal stem cells enhance vascular network formation on three-dimensional constructs in vitro. *Stem Cell Res Ther* 2016;**7**:5.

Garcia AJ, Vega MD, Boettiger D. Modulation of cell proliferation and differentiation through substrate-dependent changes in fibronectin conformation. *Mol Biol Cell* 1999;**10**:785–798.

Garimella MG, Kour S, Piprode V, Mittal M, Kumar A, Rani L, Pote ST, Mishra GC, Chattopadhyay N, Wani MR. Adipose-derived mesenchymal stem cells prevent systemic bone loss in collagen-induced arthritis. *J Immunol* 2015;**195**:5136–5148.

Germain L, De Berdt P, Vanacker J, Leprince J, Diogenes A, Jacobs D, Vandermeulen G, Bouzin C, Preat V, Dupont-Gillain C *et al*. Fibrin hydrogels to deliver dental stem cells of the apical papilla for regenerative medicine. *Regen Med* 2015;**10**:153–167.

Hong SJ, Jia SX, Xie P, Xu W, Leung KP, Mustoe TA, Galiano RD. Topically delivered adipose derived stem cells show an activated-fibroblast phenotype and enhance granulation tissue formation in skin wounds. *PLoS One* 2013;**8**:e55640.

Jensen AK, Macklon KT, Fedder J, Ernst E, Humaidan P, Andersen CY. 86 successful births and 9 ongoing pregnancies worldwide in women transplanted with frozen-thawed ovarian tissue: focus on birth and perinatal outcome in 40 of these children. *J Assist Reprod Genet* 2016;**34**:325–336.

Khan N, Williams BB, Hou H, Li H, Swartz HM. Repetitive tissue pO2 measurements by electron paramagnetic resonance oximetry: current status and future potential for experimental and clinical studies. *Antioxid Redox Signal* 2007;**9**:1169–1182.

Kim SS. Fertility preservation in female cancer patients: current developments and future directions. *Fertil Steril* 2006;**85**:1–11.

Koike N, Fukumura D, Gralla O, Au P, Schechner JS, Jain RK. Tissue engineering: creation of long-lasting blood vessels. *Nature* 2004;**428**:138–139.

Lafosse A, Desmet C, Aouassar N, Andre W, Hanet MS, Beauloye C, Vanwijck R, Poirel HA, Gallez B, Dufrane D. Autologous adipose stromal cells seeded onto a human collagen matrix for dermal regeneration in chronic wounds: clinical proof of concept. *Plast Reconstr Surg* 2015; **136**:279–295.

Lee WY, Park KJ, Cho YB, Yoon SN, Song KH, Kim DS, Jung SH, Kim M, Yoo H-W, Kim I, Ha H *et al*. Autologous adipose tissue-derived stem cells treatment demonstrated favorable and sustainable therapeutic effect for Crohn's fistula. *Stem Cells* 2013;**31**:2575–2581.

Luyckx V, Dolmans MM, Vanacker J, Legat C, Fortuno Moya C, Donnez J, Amorim CA. A new step toward the artificial ovary: survival and proliferation of isolated murine follicles after autologous transplantation in a fibrin scaffold. *Fertil Steril* 2014;**101**:1149–1156.

Mahmoodi M, Soleimani Mehranjani M, Shariatzadeh SM, Eimani H, Shahverdi A. Effects of erythropoietin on ischemia, follicular survival, and ovarian function in ovarian grafts. *Reproduction* 2014;**147**:733–741.

Mahmoodi M, Soleimani Mehranjani M, Shariatzadeh SM, Eimani H, Shahverdi A. N-acetylcysteine improves function and follicular survival in

mice ovarian grafts through inhibition of oxidative stress. *Reprod Biomed Online* 2015;**30**:101–110.

Mendel TA, Clabough EB, Kao DS, Demidova-Rice TN, Durham JT, Zotter BC, Seaman SA, Cronk SM, Rakoczy EP, Katz AJ *et al*. Pericytes derived from adipose-derived stem cells protect against retinal vasculopathy. *PLoS One* 2013;**8**:e65691.

Moon MH, Kim SY, Kim YJ, Kim SJ, Lee JB, Bae YC, Sung SM, Jung JS. Human adipose tissue-derived mesenchymal stem cells improve postnatal neovascularization in a mouse model of hindlimb ischemia. *Cell Physiol Biochem* 2006;**17**:279–290.

Nisolle M, Casanas-Roux F, Qu J, Motta P, Donnez J. Histologic and ultrastructural evaluation of fresh and frozen-thawed human ovarian xenografts in nude mice. *Fertil Steril* 2000;**74**:122–129.

Rubina K, Kalinina N, Efimenko A, Lopatina T, Melikhova V, Tsokolaeva Z, Sysoeva V, Tkachuk V, Parfyonova Y. Adipose stromal cells stimulate angiogenesis via promoting progenitor cell differentiation, secretion of angiogenic factors, and enhancing vessel maturation. *Tissue Eng Part A* 2009;**15**:2039–2050.

Shikanov A, Zhang Z, Xu M, Smith RM, Rajan A, Woodruff TK, Shea LD. Fibrin encapsulation and vascular endothelial growth factor delivery promotes ovarian graft survival in mice. *Tissue Eng Part A* 2011;**17**:3095–3104.

Soares M, Sahrari K, Chiti MC, Amorim CA, Ambroise J, Donnez J, Dolmans MM. The best source of isolated stromal cells for the artificial ovary: medulla or cortex, cryopreserved or fresh? *Hum Reprod* 2015;**30**:1589–1598.

Staff NP, Madigan NN, Morris J, Jentoft M, Sorenson EJ, Butler G, Gastineau D, Dietz A, Windebank AJ. Safety of intrathecal autologous adipose-derived mesenchymal stromal cells in patients with ALS. *Neurology* 2016;**87**:2230–2234.

Su J, Ding L, Cheng J, Yang J, Li X, Yan G, Sun H, Dai J, Hu Y. Transplantation of adipose-derived stem cells combined with collagen scaffolds restores ovarian function in a rat model of premature ovarian insufficiency. *Hum Reprod* 2016;**31**:1075–1086.

Sun M, Wang S, Li Y, Yu L, Gu F, Wang C, Yao Y. Adipose-derived stem cells improved mouse ovary function after chemotherapy-induced ovary failure. *Stem Cell Res Ther* 2013;**4**:80.

Van Eyck AS, Bouzin C, Feron O, Romeu L, Van Langendonckt A, Donnez J, Dolmans MM. Both host and graft vessels contribute to revascularization of xenografted human ovarian tissue in a murine model. *Fertil Steril* 2010;**93**:1676–1685.

Van Eyck AS, Jordan BF, Gallez B, Heilier JF, Van Langendonckt A, Donnez J. Electron paramagnetic resonance as a tool to evaluate human ovarian tissue reoxygenation after xenografting. *Fertil Steril* 2009;**92**:374–381.

Veriter S, Andre W, Aouassar N, Poirel HA, Lafosse A, Docquier PL, Dufrane D. Human adipose-derived mesenchymal stem cells in cell therapy: safety and feasibility in different 'Hospital Exemption' clinical applications. *PLoS One* 2015;**10**:e0139566.

Veriter S, Gianello P, Igarashi Y, Beaurin G, Ghyselinck A, Aouassar N, Jordan B, Gallez B, Dufrane D. Improvement of subcutaneous bioartificial pancreas vascularization and function by coencapsulation of pig islets and mesenchymal stem cells in primates. *Cell Transplant* 2014;**23**:1349–1364.

Wallace WH, Smith AG, Kelsey TW, Edgar AE, Anderson RA. Fertility preservation for girls and young women with cancer: population-based validation of criteria for ovarian tissue cryopreservation. *Lancet Oncol* 2014;**15**:1129–1136.

Xia X, Yin T, Yan J, Yan L, Jin C, Lu C, Wang T, Zhu X, Zhi X, Wang J *et al*. Mesenchymal stem cells enhance angiogenesis and follicle survival in human cryopreserved ovarian cortex transplantation. *Cell Transplant* 2015;**24**:1999–2010.

Yong KW, Pingguan-Murphy B, Xu F, Abas WA, Choi JR, Omar SZ, Azmi MA, Chua KH, Wan Safwani WK. Phenotypic and functional characterization of long-term cryopreserved human adipose-derived stem cells. *Sci Rep* 2015;**5**:9596.

Zhang Q, Wang SM, Yao PB, Zhang L, Zhang YJ, Chen RX, Fu Y, Zhang JM. Effects of L-carnitine on follicular survival and graft function following autotransplantation of cryopreserved-thawed ovarian tissues. *Cryobiology* 2015;**71**:135–140.

Zuk PA, Zhu M, Mizuno H, Huang J, Futrell JW, Katz AJ, Benhaim P, Lorenz HP, Hedrick MH. Multilineage cells from human adipose tissue: implications for cell-based therapies. *Tissue Eng* 2001;**7**:211–228.